Variation of Important Non-Dimensional Numbers During Bubble Growth at Nucleation Site in Microchannels

Sambhaji T. KADAM[1], Ritunesh KUMAR[1,] *

*Corresponding author: Tel.: (+91) 7324 240734; Fax: (+91) 7324 240761; Email: ritunesh@iiti.ac.in
1 Mechanical Engineering Department, Indian Institute of Technology Indore, MP, India

Abstract Two phase flow initiates at Onset of Nucleate Boiling, where the first bubble emerges in the downstream flow direction. Bubble nucleation and growth in microchannel heat sinks is very conspicuous phase as the growing bubble can completely block the flow cross-section area at high heat flux. Hence, microchannels are more susceptible to flow boiling instability. In this paper effort has been put to study the bubble dynamics during bubble growth at nucleation site for microchannel in terms of non-dimensional energy ratio numbers and their variation from bubble inception until departure. New non dimensional energy ratio is also proposed, which can be useful to differentiate inertia controlled and thermal diffusion controlled region during bubble growth at nucleation site.

Keywords: Microchannel, Bubble growth, Nucleation site, Non-dimensional numbers

1. Introduction

Microchannels are finding extensive range of applications due to superior heat transfer characteristics such as in microelectronics (Mudawar, 2001; Ali, 2010), advanced military avionics (Lee and Mudawar, 2008), laser mirror (Phillips, 1988), turbine blades, refrigeration cooling, thermal control in microgravity and capillary pump loops (Mudawar, 2011). Combined effect of high surface area to volume ratio and very low thermal resistance facilitate better heat transfer performance of microchannels in comparison to conventional size channels. First time, Tuckerman and Pease (1981) had developed microchannel heat sink for cooling purpose of high speed Very-large-scale integration (VLSI) circuit. He showed that microchannels based heat sink can successfully remove heat flux up to the rate of 790 W/cm^2. Further, Kandlikar (2005) postulated that enhanced microchannel geometry can successfully dissipate heat rate up to 1000 W/cm^2. Due to superior heat transfer characteristics of the two phase flow, it was extensively explored even in microchannels by many researchers (Ali, 2010; Lee and Mudawar, 2008; Mudawar, 2011; Das et al., 2012; Kandlikar, 2012; Kandlikar et al., 2012). With increase in the range of applications of microchannel heat sink, more efforts are required for comprehensive understanding of the flow boiling mechanism in microchannels. Bubble dynamics during two phase flow in microchannels governs the heat transfer, pressure drop characteristics and associated instabilities. Hence, accurate prediction of heat transfer, pressure drop and associated instabilities rely on how accurately we can predict regarding formation of bubble at nucleation sites, growth, departure and its motion along the fluid.

In conventional channel as explained by Thome (2004), the sequence of flow is bubbly, slug, churn, wispy-annular and annular flow in vertical channel flow and in the horizontal channel, bubbly, slug, plug, annular, stratified, annular with mist and wave flow exists. However, in case of the microchannels flow pattern and associated heat transfer characteristics are quite different than conventional channels. Thus, only some of the available macroscale knowledge can be applied to the microscale (Kew and Cornwell, 1997; Kandlikar, 2002). Saturated flow boiling in microchannels is governed by the nucleate boiling mechanism and the forced convection

boiling mechanism (Collier and Thome, 1994). In the nucleate boiling mechanism, heat transfer is controlled by the formation of the vapor bubble at nucleation site, which further depends on density of nucleation sites, and frequency of bubble formation (Kuo et al., 2006). Hence, bubbles inception, growth and departure are imporat aspects from the nucleate boiling prospects. Bubble growth at nucleation site is divided between two regions; inertia controlled region and diffusion controlled region (Lee et al., 2004; Bogojevic et al., 2013). In early stage during inertia controlled region, bubble is surrounded by the liquid with higher degree of superheat near heated wall of the channel. In the inertia controlled region, bubble growth is governed by the reaction force of the surrounding liquid on bubble interface. During inertia controlled region bubble growth is rapid. In later stage, bubble becomes large and its growth requires extensive evaporation of the liquid at the interface. Thus, bubble growth in later stage is governed by the thermal diffusion. In this stage bubble growth is slower than that in the inertia controlled case as the bubble is surrounded by liquid with lower superheat.

Various non-dimensional numbers (such as Martenelli parameter, Convection number, Boiling number, Bond number, Eotvos number, Capillary number, Ohnesorge number, Weber number and Jacob number) are used effectively in flow boiling. Significance of these numbers from two phase boiling prospects are explained by Kandlikar (2004). However, not all these numbers govern the performance of microchannel heat sink. Commonly useful non-dimensional numbers in case of microchannel are K_1, K_2, capillary number (Ca), Weber number (We) and Jacob number (Ja). K_1 is the ratio of evaporation momentum force and inertia force. K_2 is the ratio of evaporation momentum and surface tension force. Kandlikar (2004) also showed that K_1 and K_2 values at terminal condition can be used for predicting the critical heat flux (CHF) for flow boiling in microchannel. However, all these numbers were derived in terms of channel dimension and their variation was not studied during the entire bubble growth period. Lee and Mudawar (2005) and Bertsch et al. (2009) developed heat transfer correlation for the flow boiling in microchannel in terms of Boiling number, Weber number and Reynolds number.

In this article, effort has been made to distinguish between inertia controlled region and thermal diffusion controlled region through non dimensional number during bubble growth at nucleation site. Also, aforementioned non-dimensional energy ratio numbers variations from inception until departure are studied.

2. Energy Based Bubble Growth Model

Kadam et al. (2014) developed energy based model to predict bubble growth at nucleation site in case of microchannels. This model was based on the assumption that heat supplied at the nucleation site is divided between liquid phase and vapor phase as per instantaneous void fraction value. Thus, heat supplied at nucleation cavity was given by:

$$= q''\left(1-\varepsilon_i\right) A_c + q''\varepsilon_i\, A_c \qquad (1)$$

The first term represent the heat carried away by the liquid phase and second term indicates the heat carried away by the vapor phase. The heat carried away by the vapor phase was utilized in bubble growth (E_{bubble}) and for overcoming various resistive effects such as surface tension (Er_{sf}), inertia (Er_i), shear (Er_{sh}), gravity (Er_g) and change in momentum (Er_m) due to evaporation as shown in Fig. 1 by Eq. 2.

$$q''\varepsilon_i \cdot A_c = E_{bubble} + Er_{sf} + Er_i + Er_{sh} + Er_g + Er_m \qquad (2)$$

Energy required for bubble growth and overcoming various resistive effects was given by Eq. (3-8).

$$E_{bubble} = \rho_v h_{fg} \frac{dV_i}{dt} \qquad (3)$$

$$Er_{sf} = \sigma \frac{dA_{i,s}}{dt} \qquad (4)$$

$$\dot{E}r_i = \frac{G^2}{\rho_l} A_{i,c/s} \frac{dr}{dt} \quad (5)$$

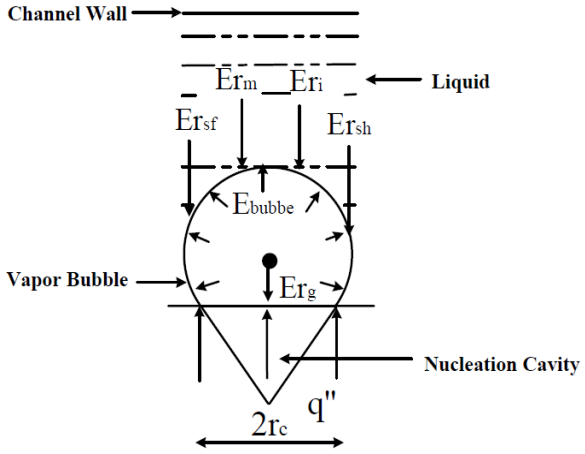

Fig. 1. Energy distribution at nucleation site (Kadam et al., 2014).

$$Er_{sh} = \mu \frac{G}{2\rho_l r} \frac{A_{i,s}}{2} \frac{dr}{dt} \quad (6)$$

$$Er_g = g\left(\rho_l - \rho_v\right) \cdot a \frac{dV_i}{dt} \quad (7)$$

$$Er_m = \frac{q''}{h_{fg}} A_{i,s} \frac{q''}{h_{fg}\rho_v} \frac{dr}{dt} \quad (8)$$

The instantaneous volume (V_i), surface area ($A_{i,s}$), cross sectional area ($A_{i,c/s}$) and centroid (a) of the bubble were derived in terms of contact angle and bubble radius. The shape of the bubble was assumed as a truncated sphere as shown in Fig. 2. Instantaneous volume, surface area and cross sectional area of the bubble were given by Eq. (9), Eq. (10) and Eq. (11), respectively.

$$V_i = \frac{\pi}{3} \cdot r^3 \alpha \quad (9)$$

$$A_{i,s} = \pi \cdot r^2 \cdot \beta \quad (10)$$

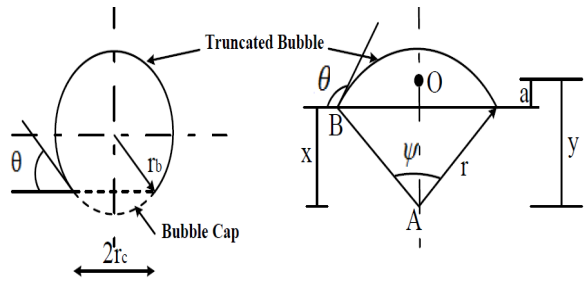

Fig. 2. Diagram of truncated bubble and centroid of the bubble.

$$A_{i,c/s} = \frac{1}{2} \cdot r^2 \gamma \quad (11)$$

Where, α, γ and β were given by Eq. (12-14).

$$\alpha = \left[4 - 0.5\left\{3(1-\cos\theta)\sin^2\theta + (1-\cos\theta)^3\right\}\right] \quad (12)$$

$$\beta = \left[4 - \left\{\sin^2\theta + (1-\cos\theta)^2\right\}\right] \quad (13)$$

$$\gamma = \left[2\pi - \frac{2\pi\theta}{180} + \sin 2\theta\right] \quad (14)$$

The location of the centroid of the bubble is shown in Fig. 2 at point 'o'. The distance between centroid of the bubble and plate was given by Eq. (15).

$$a = y - x = r\left[\frac{4\sin^3\left(\frac{\psi}{2}\right)}{3(\psi - \sin\psi)} - \sin\left(90 - \frac{\psi}{2}\right)\right] = r\varphi \quad (15)$$

Where, ψ and ϕ were given by Eq. (16-17).

$$\psi = 2(180 - \theta) \quad (16)$$

$$\phi = \left[\frac{4\sin^3\left(\frac{\psi}{2}\right)}{3(\psi - \sin\psi)} - \sin\left(90 - \frac{\psi}{2}\right)\right] \quad (17)$$

Substituting Eq. (3-8) into the Eq. (2), the bubble growth rate is given by Eq. (18).

$$q'' \frac{A_c}{A_{ch}} \frac{\gamma}{2} r^2 = r^2 \frac{dr}{dt}\left[\pi \cdot \alpha \cdot \rho_v h_{fg} + \frac{G^2}{2\rho_l}\gamma + \left(\frac{q''}{h_{fg}}\right)^2 \frac{\pi \cdot \beta}{\rho_v}\right] + r \cdot \frac{dr}{dt}\left[\sigma \cdot (2 \cdot \pi \cdot \beta) + \mu \frac{G}{4 \cdot \rho_l} \pi \cdot \beta\right] + r^3 \frac{dr}{dt}\left[g\left(\rho_l - \rho_v\right)\frac{\pi \cdot \alpha \cdot \phi}{2}\right] \quad (18)$$

Kadam et al. (2014) had shown that solution of Eq. (18) predicts the growth of bubble growth at nucleation site with good accuracy. In order to find important energy non-dimensional numbers, first variation of different components of this equation are studied during the entire growth period since inception to departure.

3. **Non-Dimensional Group**

Fig. 3 shows the variation of E_{bubble}, Er_{sf}, Er_i, Er_{sh}, Er_g and Er_m following experimental study of Li et al. (2004). It can be observed that the energy required to overcome resistive effect of evaporation momentum is negligible out of these.

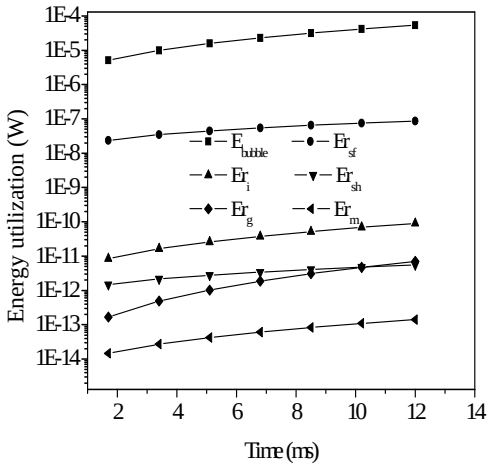

Fig. 3. Variation of energy utilization in various effects during bubble growth (Li et al., 2004) for G=105 kg/m^{2}s, q"=121 kW/m^2.

Hence, this effect has not been considered in current non-dimensional study. Following that, E_{bubble}, Er_{sf}, Er_i, Er_{sh}, and Er_g are remaining influencing parameters in Eq. 2. During current analysis, energy required to overcome the surface tension effect has been taken as reference as it plays important role in bubble growth and departure both in microchannels. Four dimensionless energy ratio terms have been formed as: E_1, E_2, E_3 and E_4 as shown by Eq. (19-22).

$$E_1 = E_{bubble} \Big/ Er_{sf} = \frac{\rho_v h_{fg}}{2\sigma} r \frac{\alpha}{\beta} \tag{19}$$

$$E_2 = Er_i \Big/ Er_{sf} = \frac{r\,G^2}{\rho_l \sigma}\left(\frac{\gamma}{4\pi\beta}\right) = We\left(\frac{\gamma}{4\pi\beta}\right) \tag{20}$$

$$E_3 = Er_{sh} \Big/ Er_{sf} = \frac{\mu\, G}{8\rho_l \sigma} = \frac{Ca}{8} \tag{21}$$

$$E_4 = Er_g \Big/ Er_{sf} = \frac{g\left(\rho_l - \rho_g\right)}{2\sigma} r^2 \left(\frac{\varphi\alpha}{\beta}\right) = \frac{Bo}{2}\left(\frac{\varphi\alpha}{\beta}\right) \tag{22}$$

Where, $We\left(=\frac{r\,G^2}{\rho_l\sigma}\right)$ is Weber number, $Ca\left(=\frac{\mu\, G}{\rho_l\sigma}\right)$ is Capillary number, $Bo\left(=\frac{g\left(\rho_l-\rho_g\right)}{\sigma} r^2\right)$ is Bond number.

Where, E_1 is the ratio of the energy required for bubble growth to the energy required to overcome the surface tension effect. E_2 is the ratio of the energy required to overcome the inertia effect to the surface tension effect. It finally appears in terms of the Weber number. E_3 is the ratio of energy required to overcome shear effect and surface tension effect. E_3 is function of the capillary number. E_4 is the ratio of the energy required to overcome the gravity (buoyancy) effect to the surface tension effect. It appears in terms of the Bond number.

4. **Result & Discussion**

Many researchers had carried out experimental studies of bubble growth at nucleation site (Li et al. 2004; Lee, 2004; Liu et al., 2005; Wang et al., 2006; Meder, 2007) in microchannels. But, they had not observed inertia controlled region and thermal diffusion controlled region distinctly in their experimental studies. They reported that bubble grows at nucleation site in linear manner. Only single experimental data of Bogojevic et al. (2013) was found in the open literature, which clearly indentifies the inertia controlled and thermal diffusion controlled region separately during bubble growth at

nucleation site in microchannel.

Following Bogojevic et al. (2013) study, it is observed that period of the inertia controlled region is very short as compared to thermal diffusion controlled region. This could be a possible reason that in rest of earlier experimental studies this region could not be identified or may be due to limitation of high speed photography they could not detect it. The above mentioned non-dimensional groups are plotted following instantaneous values of bubble radius (since inception till departure) as reported in experimental work of the Bogojevic et al. (2013). Fig. 4-7 shows the variation of E_1, E_2, E_3 and E_4 *during the entire bubble life.*

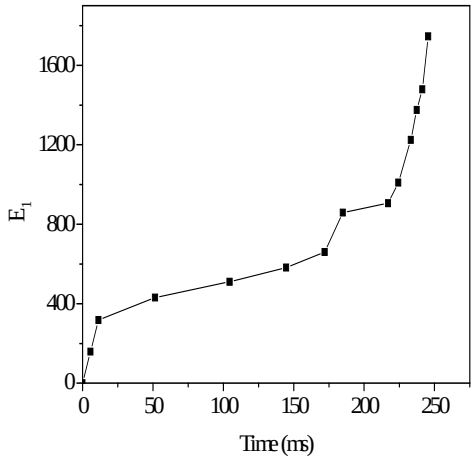

Fig. 4. Variation of the E_1 with time.

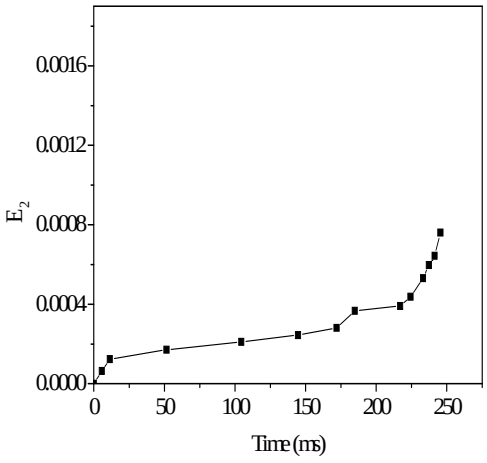

Fig. 5. Variation of the E_2 with time.

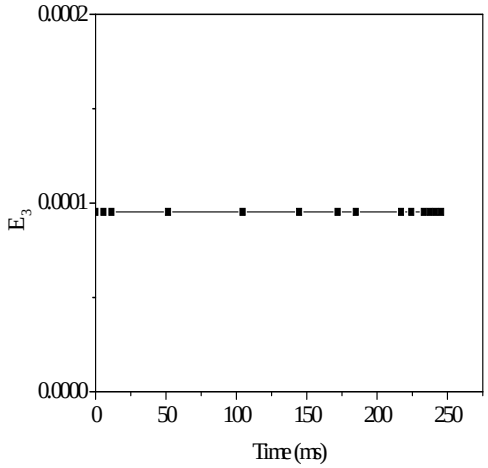

Fig. 6. Variation of the E_3 with time.

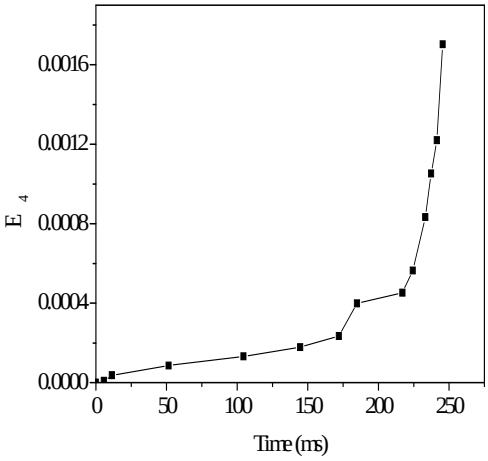

Fig. 7. Variation of the E_4 with time.

It is clear from these figures that E_1 and E_2 play important role in bubble growth at nucleation site. E_3 does not change with time during entire bubble growth at nucleation site as shown in Fig. 6. The effect of E_4 is not important as for as inertia controlled and thermal diffusion controlled regions are concerned. Unlike E_1 and E_2, variation of E_4 is almost linear during combined region. Hence, gravitation force does not play any significant role in these regions. Variation of E_1 and E_2 show that they can be utilized to distinguish the inertia controlled and thermal diffusion controlled region. E_2 appears in terms of the

We, which is useful in defining the dominance of the surface tension and flow inertia on flow patterns in microchannel (Kandlikar, 2004). Thus, E_1 is most meaningful for differentiating inertia controlled region and diffusion controlled region. It consists of the surface tension term, which is dominating in early stage of the bubble growth and latent heat of the evaporation, which plays an important role in later stage of the bubble growth.

Initially the value of E_1 increases very rapidly and attains value of around 400 within a short time (around 25 ms). In this region bubble size is very small thus surface tension effect plays an important role. Later, the slope of the curve reduces as the bubble size increases. In this region, evaporation is mainly responsible for further growth of bubble as surface tension effects turns weaker. Thus, bubble growth in this region is governed by the thermal diffusion taking place at the liquid vapor interface. Hence, variation of E_1 can be used successfully for easily recognizing inertia controlled region and diffusion controlled regions.

From the Fig. 4 it is clear that rate of bubble growth is much higher in inertia controlled region than thermal diffusion controlled region. Hence, it implies that rate of the heat transfer from the surface is much higher to fluid in the inertia controlled region than the thermal diffusion controlled region. If the bubble can be departed before it enters into thermal diffusion controlled region, higher heat transfer rate can be achieved.

5. **Conclusion**

In this paper, bubble dynamics at nucleation site is discussed in terms of the non dimensional energy ratios. To differentiate inertia controlled region and thermal diffusion controlled region, a new non dimensional energy ratio number E_1 has been proposed, which is a ratio of the energy required for bubble growth to the energy required to overcome surface tension effect. It is found that inertia controlled region remains dominant until E_1 is less than 400. Further efforts are required to generalize this transition criterion.

Nomenclature

A = area (m^2)
a = bubble centroid (m)
D = channel diameter (m)
E = non-dimensional energy ratio parameter
Er = energy required to overcome resistive effect (W)
g = acceleration due to gravity (m^2/s)
G = mass flux (kg/m^2s)
h_{fg} = latent heat (J/kg)
r = bubble radius (m)
q'' = effective heat supplied to channel (W/m^2)
t = time (s)
V = bubble volume (m^3)

Greek

ρ_l = liquid density (kg/m^3).
ρ_v = vapor density (kg/m^3).
μ = viscosity ($N\ s/m^2$)
θ = contact angle (º)
σ = surface tension (N/m)

Subscript:

ch = channel cross section
c/s = bubble cross section
i = inertia, instantaneous value when used with volume and areas
s = bubble surface
sf = surface tension
sh = shear
m = evaporation momentum

References:

Ali, R., 2010. Phase change phenomena during fluid flow in micro channels. Ph.D. Thesis, Royal Institute of Technology, Stockholm, Sweden.

Bertsch, S. S., Groll, E. A., Garimella, S. V., 2009. A composite heat transfer correlation for saturated flow boiling in small channels, Int. J. Heat Mass Transfer 52, 2110– 2118.

Bogojevic, D., Sefiane, K., Duursma, G., Walton, A. J., 2013. Bubble dynamics and flow boiling instabilities in microchannel. Int. J. Heat Mass Tran. 58, 663–675.

Collier, J. G., Thome, J. R., 1994. Convective boiling and condensation. Third ed., Oxford University Press, Oxford.

Das, P. K., Chakraborty, S., Bhaduri, S., 2012. Critical heat flux during flow boiling in mini and microchannel- a state of the art review.

Frontiers in Heat Mass Transfer 3, 1-17.
Kadam, S. T., Kumar, R., and Baghel, K. 2014. Simplified model for prediction of bubble growth in microchannels. ASME J. Heat Transfer 136, 1-8.
Kandlikar, S. G., 2002. Fundamental issues related to flow boiling in minichannels and microchannels. Exp. Therm. Fluid Sci. 26, 389‑407.
Kandlikar S. G., 2004. Heat transfer mechanism during flow boiling in microchannels. J. Heat Trans. 126, 8-16.
Kandlikar, S. G., 2005. High flux heat removal with microchannels- a roadmap of challenges and opportunities. Heat Trans. Engg. 26, 5-14.
Kandlikar, S. G., 2012. History, advances and challenges in liquid flow and flow boiling heat transfer in microchannels: a critical review. J. Heat Trans. 134, 034001-1.
Kandlikar, S. G., Colin, S., Peles, P., Garimella, S., Pease, R. F., Brandner, J. J., Tuckerman, D. B., 2012. Heat transfer in microchannels—2012 status and research needs. J. Heat Trans. 135, 091001-1.
Kew, P. A., and Cornwell, K., 1997. Correlations for the prediction of boiling heat transfer in small-diameter channels. Applied Therm. Engg. 17, 705-715.
Kuo, C. J., Kosar, A., Peles, Y., Virost, S., Mishra, C., and Jensen M. K., 2006. Bubble dynamics during boiling in enhanced surface microchannels. J. Microelectromechanical Systems 15, 1514-1527.
Lee, P.C., Tseng, F.G., and Pan, C., 2004. Bubble dynamics in microchannels. part i: single microchannel. Int. J. Heat Mass Transfer 47, 5575–5589.
Lee, J. Mudawar, I., 2005. Two-phase flow in high-heat-flux micro-channel heat sink for refrigeration cooling applications: Part II—heat transfer characteristics. Int. J. Heat and Mass Transfer 48, 941–955.
Lee, J., Mudawar, I., 2008. Fluid flow and heat transfer characteristics of low temperature two-phase microchannel heat sink – part1: experimental methods and flow visualization results. Int. J. Heat Mass Transfer 51, 4315-4326.
Li, H.Y., Tseng, F.G., Pan, C., 2004. Bubble dynamics in microchannels. Part II: Two Parallel Microchannels. Int. J. Heat Mass Transfer 47, 5591–5601.
Liu, D., Lee, P. S., Garimella, S. V., 2005. Prediction of the onset of nucleate boiling in microchannels flow. Int. J. Heat Mass Transfer 48, 5134–5149.
Meder, S., 2007. Study on bubble growth rate in a single microchannel heat exchanger with high-speed CMOS-camera. Master Thesis, Swiss Federal Institute of Technology Zurich and Stanford University California.
Mudawar, I., 2001. Assessment of high-heat-flux thermal management schemes. IEEE Trans. Compon. Packag. Technol. 24, 122–141.
Mudawar, I., 2011. Two-Phase microchannels heat sink: theory, application and limitation. J. Electron. Packag. 133, 1-31.
Phillips, R. J., 1988. Microchannels heat sinks. Lincoln Laboratory J. 1, 31-47.
Thome, J. R., 2004. Engineering data book III, Wolverine Tube Inc.
Tuckerman, D. B., and Pease, R. F. W., 1981. High-performance heat sinking for VLSI. IEEE Electron Device Letters 2, 126-129.
Wang, E. N., Devasenathipathy, S., Lin, H., Hidrovo, C. H., Santiago, J. G., Goodson, and K. E., Kenny, T. W., 2006. A hybrid method for bubble geometry reconstruction in two-phase microchannels. Expts. in Fluids 40, 847-858.